PNAS RESEARCH ARTICLE | NEUROSCIENCE

Mitigating aberrant Cdk5 activation alleviates mitochondrial defects and motor neuron disease symptoms in spinal muscular atrophy

Nimrod Miller[a,b,1], Zhaofa Xu[a,b,1], Katharina A. Quinlan[c,d,e,f], Amy Ji[a], Jered V. McGivern[g], Zhihua Feng[h], Han Shi[a,b], Chien-Ping Ko[h], Li-Huei Tsai[i], Charles J. Heckman[c,d,e], Allison D. Ebert[g], and Yongchao C. Ma[a,b,c,2]

Edited by Michael Greenberg, Harvard Medical School, Boston, MA; received January 6, 2023; accepted July 31, 2023

Spinal muscular atrophy (SMA), the top genetic cause of infant mortality, is characterized by motor neuron degeneration. Mechanisms underlying SMA pathogenesis remain largely unknown. Here, we report that the activity of cyclin-dependent kinase 5 (Cdk5) and the conversion of its activating subunit p35 to the more potent activator p25 are significantly up-regulated in mouse models and human induced pluripotent stem cell (iPSC) models of SMA. The increase of Cdk5 activity occurs before the onset of SMA phenotypes, suggesting that it may be an initiator of the disease. Importantly, aberrant Cdk5 activation causes mitochondrial defects and motor neuron degeneration, as the genetic knockout of *p35* in an SMA mouse model rescues mitochondrial transport and fragmentation defects, and alleviates SMA phenotypes including motor neuron hyperexcitability, loss of excitatory synapses, neuromuscular junction denervation, and motor neuron degeneration. Inhibition of the Cdk5 signaling pathway reduces the degeneration of motor neurons derived from SMA mice and human SMA iPSCs. Altogether, our studies reveal a critical role for the aberrant activation of Cdk5 in SMA pathogenesis and suggest a potential target for therapeutic intervention.

Cdk5 | spinal muscular atrophy | motor neuron | mitochondria | neurodegeneration

SMA (spinal muscular atrophy) is an autosomal recessive genetic disorder characterized by motor neuron degeneration, which leads to muscle atrophy, paralysis, and death (1–5). As the primary genetic cause of infant mortality, SMA is caused by loss-of-function mutations in the *Survival Motor Neuron1* (*SMN1*) gene, leading to reduced SMN protein level and ultimately motor neuron degeneration (6–10). SMN has been implicated in diverse functional processes including snRNP (small nuclear ribonucleoprotein) biogenesis and pre-mRNA splicing (11–17). Spinal motor neurons affected by SMA exhibit defects including mitochondrial dysfunction, loss of excitatory synapse innervation, and NMJ (neuromuscular junction) denervation before undergoing neurodegeneration (18–23). Although SMN-up-regulating treatments have been developed (24–26), significant limitations exist (27), and mechanisms underlying motor neuron degeneration in SMA remain largely elusive.

Cyclin-dependent kinase 5 (Cdk5) is a proline-directed serine/threonine kinase that controls a wide range of functions in the nervous system, including neuronal migration, synaptic transmission, NMJ function, axonal transport, and neuronal survival (28–42). Dysregulation of Cdk5 activity has been implicated in a number of neurodegenerative disorders including Alzheimer's disease, Parkinson's disease, and Niemann Pick type C disease (34, 43–46). The kinase activity of Cdk5 is tightly regulated by the expression and localization of its activating regulatory subunits p35 and p39 (39, 40, 47, 48). Although Cdk5 protein is ubiquitously expressed in all cell types, Cdk5 kinase activity is mainly detected in postmitotic neurons, as a result of the neuron-specific expression of its activating subunits (49, 50). P35 can be cleaved by the Ca^{2+}-dependent protease calpain to generate p25 (51, 52), which has a substantially longer half-life than that of p35 and also lacks a membrane-binding myristylation site. Thus, the binding of p25 to Cdk5 causes hyperactivation and increased non-membrane localization of Cdk5 (51, 52). Under pathological circumstances such as Alzheimer's disease, increased p25 level and enhanced Cdk5 kinase activity lead to protein aggregation and neurodegeneration (53, 54). Genetic knockout studies in mice revealed that Cdk5 regulated many motor neuron-related functions, including motor axon projection, NMJ function, and motor neuron degeneration, which are also defective in SMA (35, 55). We also found that the phosphorylation of microtubule-associated protein tau by Cdk5 was significantly increased in SMA patient samples and mouse models (56). These findings suggest that Cdk5 may play a critical role in SMA pathogenesis, a possibility that has not been thoroughly investigated.

Significance

Pathogenic mechanisms underlying spinal muscular atrophy (SMA), the top genetic killer of toddlers, are not known. Here, we report that cyclin-dependent kinase 5 (Cdk5) is aberrantly activated in mouse and human induced pluripotent stem cell (iPSC) models of SMA before the onset of disease symptoms. Reducing Cdk5 activity genetically in an SMA mouse model rescues mitochondrial defects and significantly alleviates disease phenotypes in mice. These findings reveal a novel mechanism involving the upregulation of Cdk5 activity in SMA pathogenesis. In addition, inhibition of Cdk5 signaling decreases the degeneration of motor neurons derived from SMA mice and human SMA iPSC disease models, suggesting that reducing aberrant Cdk5 activation can potentially ameliorate SMA disease symptoms and benefit patients.

Author contributions: N.M. and Y.C.M. designed research; N.M., Z.X., K.A.Q., A.J., J.V.M., Z.F., H.S., and Y.C.M. performed research; L.-H.T. contributed reagents; N.M., Z.X., K.A.Q., A.J., J.V.M., Z.F., H.S., C.-P.K., C.J.H., A.D.E., and Y.C.M. analyzed data; and Y.C.M. wrote the paper.

The authors declare no competing interest.

This article is a PNAS Direct Submission.

[1]N.M. and Z.X. contributed equally to this work.

[2]To whom correspondence may be addressed. Email: ma@northwestern.edu.

This article contains supporting information online at https://www.pnas.org/lookup/suppl/doi:10.1073/pnas.2300308120/-/DCSupplemental.

Published November 17, 2023.

Here, we report that the activity of Cdk5 kinase is significantly up-regulated before the onset of disease symptoms in SMA mouse models and human iPSC (induced pluripotent stem cell) models, suggesting a role for Cdk5 aberrant activation in initiating SMA pathogenesis. We also show that Cdk5 hyperactivation causes mitochondrial defects and motor neuron degeneration, as the genetic knockout of Cdk5 activating subunit *p35* in SMA mice rescues mitochondrial defects and significantly improves SMA disease phenotypes including motor neuron hyperexcitability, excitatory synapse loss on motor neurons, motor axon denervation at NMJs, and motor neuron degeneration. Additionally, mitigating aberrant Cdk5 activation reduces degeneration of motor neurons derived from SMA mice and human SMA iPSCs. Altogether, our findings reveal a critical role for the aberrant upregulation of Cdk5 activity in SMA pathogenesis and suggest a potential therapeutic strategy.

Results

Aberrant Activation of Cdk5 Kinase in SMA Mice Before the Onset of Disease Symptoms. Increased Cdk5 kinase activity has been implicated in a number of neurodegenerative disorders (34, 43, 44). Because SMA is characterized by spinal motor neuron degeneration, we examined whether the activity of Cdk5 kinase is dysregulated in SMA disease conditions. We utilized two widely used SMA mouse models, the Δ7 SMA mice (*Smn*$^{-/-}$;*SMN2*$^{tg/tg}$;*SMNΔ7*$^{tg/tg}$) (57) and the Hung-Li SMA mice (*Smn*$^{-/-}$;*SMN2Hung*$^{tg/-}$) (58). These mouse models express different forms of human *SMN2* transgene on the mouse *Smn* knockout background. Disease mice have an average life span of approximately 13 d and exhibit symptoms and neuropathology similar to patients afflicted with severe forms of SMA (57, 58). Using the Δ7 SMA mice, we immunoprecipitated endogenous Cdk5 kinase from spinal cord lysates and assayed its activity of phosphorylating a known Cdk5 substrate, Histone H1, with ^{32}P-γ-ATP (59, 60). We found that endogenous Cdk5 kinase activity was up-regulated in SMA mice compared to control wild-type (WT) littermates at postnatal day 9 (P9) (Fig. 1 *A* and *B*), while the amount of Cdk5 protein was at the same level (Fig. 1*A*). At P9, the Δ7 SMA mice show severe motor behavioral defects (Fig. 1 *C* and *D*) and are smaller than the WT littermates (Fig. 1*F*). Therefore, P9 has been considered as a postsymptomatic stage. To test whether the upregulation of Cdk5 kinase activity is a secondary effect to motor neuron degeneration in SMA mice, we examined Cdk5 activity at postnatal day 3 (P3). P3 is a presymptomatic stage when Δ7 SMA mice are not significantly different from their WT littermates (Fig. 1 *C–E*). We observed a substantial increase in endogenous Cdk5 kinase activity in presymptomatic P3 mice (Fig. 1 *A* and *B*), indicating that the increase of Cdk5 kinase activity is not a consequence of disease phenotypes in SMA, but instead likely contributes to the initiation of SMA pathogenesis. Similarly, we also found significantly increased endogenous Cdk5 activity in a second SMA mouse model, the Hung-Li SMA mice (Fig. 1 *G* and *H*). These observations suggest that increased Cdk5 activity is not limited to a specific SMA mouse model but is likely associated with the general SMA pathology. Furthermore, we also examined Cdk5 activity at earlier time points (E18.5) in SMA mouse models and found increased Cdk5 kinase activity although not statistically significant (*SI Appendix*, Fig. S1*A*). Taken together, these results indicate that the upregulation of Cdk5 kinase activity in the spinal cord is a conserved phenomenon that may contribute to the initiation of SMA pathogenesis.

Increased Conversion of p35 to p25 in SMA Mouse Models. The kinase activity of Cdk5 is dictated by its activating subunit p35 or p25. P35 can be cleaved by Ca^{2+}-dependent protease calpain to generate p25, which is a more potent Cdk5 activator (51, 52). Our observation that Cdk5 protein levels are not changed in SMA mice (Fig. 1 *A* and *G*) prompted us to test whether the up-regulated Cdk5 kinase activity is due to increased conversion of p35 into p25. We examined the levels of p35 and p25 in spinal cords from both the Δ7 SMA mice and the Hung-Li SMA mice by Western blot analysis. The specificity of the anti-p35/p25 antibody was confirmed on neuronal lysates from *p35* knockout mice (Fig. 2*A*). We found substantially increased p25 protein levels in spinal cords of Δ7 SMA mice and Hung-Li SMA mice (Fig. 2 *A* and *B*), compared to those of littermate control mice at P9. To test whether the upregulation of p25 occurs before SMA phenotypes, we also examined the level of p25 at the presymptomatic stage P3. We observed significantly increased p25 in P3 SMA spinal cords of both Δ7 SMA mice and Hung-Li SMA mice (Fig. 2 *A* and *B*). These data suggest that calpain-mediated conversion of p35 to p25 is also up-regulated in SMA mouse models before the onset of disease symptoms, potentially leading to aberrant Cdk5 kinase activation.

Upregulations of Cdk5 Activity and p25 Level Are Conserved in Human iPSC Models of SMA. Our findings on the increased conversion of p35 to p25 and the up-regulated Cdk5 activity in SMA mice led us to speculate that this aberrant activation of Cdk5 signaling might also exist in human SMA disease. To test this idea, we utilized iPSCs derived from human SMA patients. Patient-derived iPSCs offer unique advantages in studying disease mechanisms and performing drug screenings because of their identical genetic architecture to human patients. SMA iPSCs have been generated from skin fibroblasts of SMA patients and their unaffected relatives (61, 62). Motor neurons that express both neuronal marker TuJ1 and motor neuron marker Isl1 can be derived from Oct4-expressing pluripotent SMA iPSCs (Fig. 3 *A–F*). These SMA iPSC-derived motor neurons show increased caspase activation, motor neuron degeneration, and other disease phenotypes (61–63), serving as a human iPSC model of SMA. Consistent with results from SMA mice, immunoprecipitation kinase assay showed substantially increased endogenous Cdk5 kinase activity in motor neurons derived from SMA iPSCs generated by lentivirus-based reprogramming (Fig. 3 *G* and *I*) or by footprint-free nonintegrating episomal approach (*SI Appendix*, Fig. S1*B*) (61, 62). In addition, quantification of Western blot analysis revealed that p25 levels also increased in SMA iPSC-derived motor neurons (Fig. 3 *H* and *J*), suggesting that upregulations of Cdk5 activity and p25 level in SMA pathogenesis are likely a mechanism conserved in human patients.

Mitigating Aberrant Cdk5 Activation Reduces the Degeneration of SMA Mouse Motor Neurons. Next, we asked whether reducing aberrant Cdk5 activation in SMA conditions might serve to ameliorate motor neuron degeneration. To address this question, we monitored the degeneration of motor neurons cultured from Δ7 SMA mice and control mice by TUNEL staining. We treated these mouse motor neurons with lentivirus carrying short hairpin RNA (shRNA) to knock down Cdk5 expression, or pharmacological inhibitors to reduce Cdk5 kinase activity (Fig. 4). Isl1 and TuJ1 positive motor neurons from Δ7 SMA mice showed dramatically increased degeneration compared to those from non-disease control mice (Fig. 4*D*), while applying 300 nM Cdk5 inhibitor BML259 or shRNA-mediated *Cdk5* knockdown significantly reduced degeneration (Fig. 4*D*). These data support a critical role for aberrant Cdk5 activation in causing motor neuron degeneration in SMA.

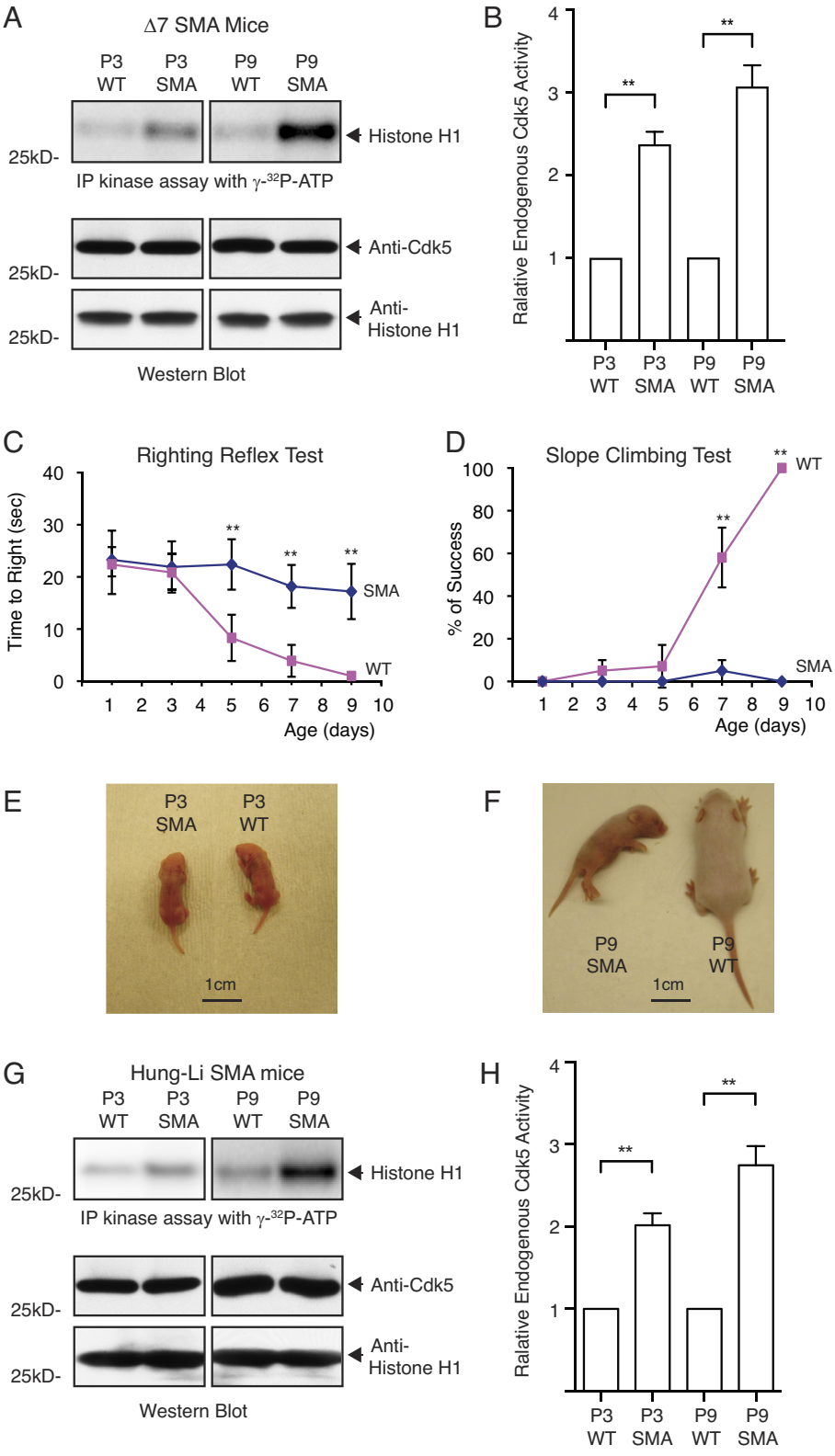

Fig. 1. Endogenous Cdk5 kinase activity is up-regulated in SMA mouse spinal cords before the onset of disease symptoms. (*A* and *B*) Cdk5 kinase activity is significantly elevated in spinal cords from Δ7 SMA mice ($Smn^{-/-};SMN2^{tg/tg};SMN\Delta7^{tg/tg}$) both at postnatal day 3 (P3) and postnatal day 9 (P9). Endogenous Cdk5 was immunoprecipitated from spinal cord lysates of P3 and P9 mice. Kinase activity of immunoprecipitated Cdk5 was measured by its phosphorylation of Histone H1 with ^{32}P-γ-ATP, shown by autoradiography in (*A*). The same levels of Cdk5 and purified Histone H1 used in kinase assay reactions were monitored by Western blotting. Kinase activity was quantified (*B*) using a phosphor imager and scintillation counter. Data are from four independent experiments and are mean ± SEM. $^{**}P < 0.01$, paired Student's *t* test. WT: wild type; SMA: spinal muscular atrophy. (*C* and *D*) Time course of motor symptom onset in SMA mice. From P5 to P9, Δ7 SMA mice (blue line, n = 21) took significantly longer to right themselves compared to WT control littermates (magenta line, n = 18) (*C*). By P7, significantly more WT control littermates (magenta line, n = 18) could successfully climb 55° incline in 1 min compared to SMA mice (blue line, n = 21) (*D*). (*E* and *F*) Relative size of SMA mice at P3 and P9. At P3 (*E*), Δ7 SMA mice and WT control mice are very similar in size, while at P9 (*F*), SMA mice are significantly smaller and less active. (*G* and *H*) Cdk5 kinase activity is also up-regulated in the Hung-Li SMA mouse model ($Smn^{-/-};SMN2Hung^{tg/-}$) Endogenous Cdk5 was immunoprecipitated from P3 and P9 spinal cord lysates, and the kinase activity was measured by its phosphorylation of Histone H1 with ^{32}P-γ-ATP. Data are from four independent experiments and are mean ± SEM. $^{**}P < 0.01$, paired Student's *t* test.

Genetic Knockout of *p35* Rescues Mitochondrial Defects in SMA Mouse Motor Neurons. To further establish the importance of Cdk5 signaling in SMA pathogenesis, we tried to test whether genetic knockout of *Cdk5* or its activating subunit *p35* can rescue functional defects in SMA. This requires the generation of compound mutant mice that carry the *Cdk5* or *p35* knockout alleles on the background of an SMA mouse model. *Cdk5* null mice are perinatal lethal (64), preventing the analysis of SMA phenotypes in postnatal mice. Therefore, we crossed *p35* null mice, which can survive into adulthood (65), with the Hung-Li SMA mouse model ($Smn^{-/-};SMN2Hung^{tg/-}$) to generate a compound $Smn^{-/-};SMN2Hung^{tg/-};p35^{-/-}$ ($SMA;p35^{-/-}$) mouse strain, and examined SMA disease phenotypes in these mice. Kinase assay showed that endogenous Cdk5 activity was significantly reduced in SMA mice by *p35* knockout (*SI Appendix*, Fig. S3). Studies from our laboratory revealed mitochondrial transport and fragmentation

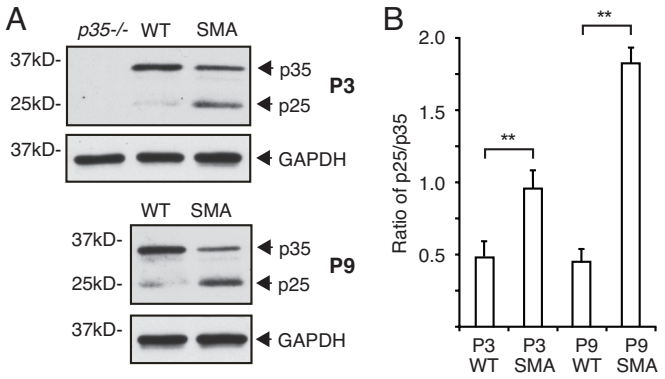

Fig. 2. Increased conversion of p35 to p25 in SMA mouse spinal cords. (*A*) Western blot analysis shows that the p25 protein level is significantly increased at both presymptomatic (P3) and postsymptomatic (P9) stages in spinal cords from Δ7 SMA mice. Neither p35 nor p25 was detected in *p35* knockout mice ($p35^{-/-}$). Expression levels of GAPDH detected by Western blotting were used as control. (*B*) Quantification of the p35 to p25 ratio in Δ7 SMA mice by measuring integrated optical density. Data are from four independent experiments and are mean ± SEM. $^{**}P < 0.01$, Student's *t* test.

defects as critical SMA disease phenotypes (22). Cdk5 has also been implicated in regulating mitochondrial transport and fission (30, 37, 66). Therefore, we tested whether genetic knockout of *p35* in SMA mice could attenuate mitochondrial transport and fragmentation defects. We used time-lapse confocal live imaging to measure mitochondrial transport and size in primary mouse motor neurons from SMA mice and $SMA;p35^{-/-}$ mice expressing DsRed tagged with mitochondria targeting sequence (mito-DsRed). Motor neurons from SMA mice exhibited a significant decrease in the number of mobile mitochondria, total mitochondrial travel distance, and retrograde transport compared to those from WT mice (Fig. 5 *A*–*H*). Notably, retrograde transport of mitochondria (Fig. 5*H*) was particularly affected in SMA motor neurons, consistent with findings that Cdk5 hyperactivation by p25 specifically disrupts dynein-mediated retrograde axonal transport (30). Importantly, all three mitochondrial transport defects were restored to WT mouse level in motor neurons from $SMA;p35^{-/-}$ compound mutant mice (Fig. 5 *A*–*H*), indicating that *p35* knockout can rescue mitochondria mobility defects in SMA. In addition to mitochondrial transport, we also examined mitochondrial size. Fragmented mitochondria exhibit decreased cristae density leading to impaired ATP synthesis, increased oxidative stress, and mitochondrial DNA leakage-induced neuroinflammation (22, 67, 68), potentially contributing to neurodegeneration. Cdk5 hyperactivation has also been associated with increased mitochondria fission and fragmentation (66). Indeed, SMA mouse motor neurons showed short and fragmented morphology compared to those from WT mice, while in $SMA;p35^{-/-}$ mice these defects were rescued to WT levels (Fig. 5 *I* and *J*). Collectively, these results show the critical role of Cdk5 hyperactivation by p25 in causing mitochondrial defects in motor neurons affected by SMA.

Genetic Knockout of *p35* Alleviates Disease Phenotypes in SMA Mice. To further investigate the role of aberrant Cdk5 activation in SMA pathogenesis in vivo, we examined other SMA disease phenotypes in $SMA;p35^{-/-}$ compound mutant mice. During SMA pathogenesis, motor neurons are characterized by the loss of excitatory synapse innervation on motor neuron cell bodies (18, 20, 56). Thus, we first tested whether genetic knockout of *p35* could rescue the excitatory synapse loss phenotype. We quantified the number of excitatory synapses on lumbar level spinal motor neurons by the colocalization of glutamatergic synapse marker vesicular glutamate transporter 1 (vGluT1) with motor neuron marker choline acetyltransferase (ChAT) (Fig. 6 *A*–*E*). The number of excitatory synaptic boutons on motor neurons showed significant reduction in SMA mice, but recovered to WT level in $SMA;p35^{-/-}$ compound mutant mice (Fig. 6 *A*–*E*), suggesting *p35* knockout rescues the excitatory synapse loss phenotype in SMA mice.

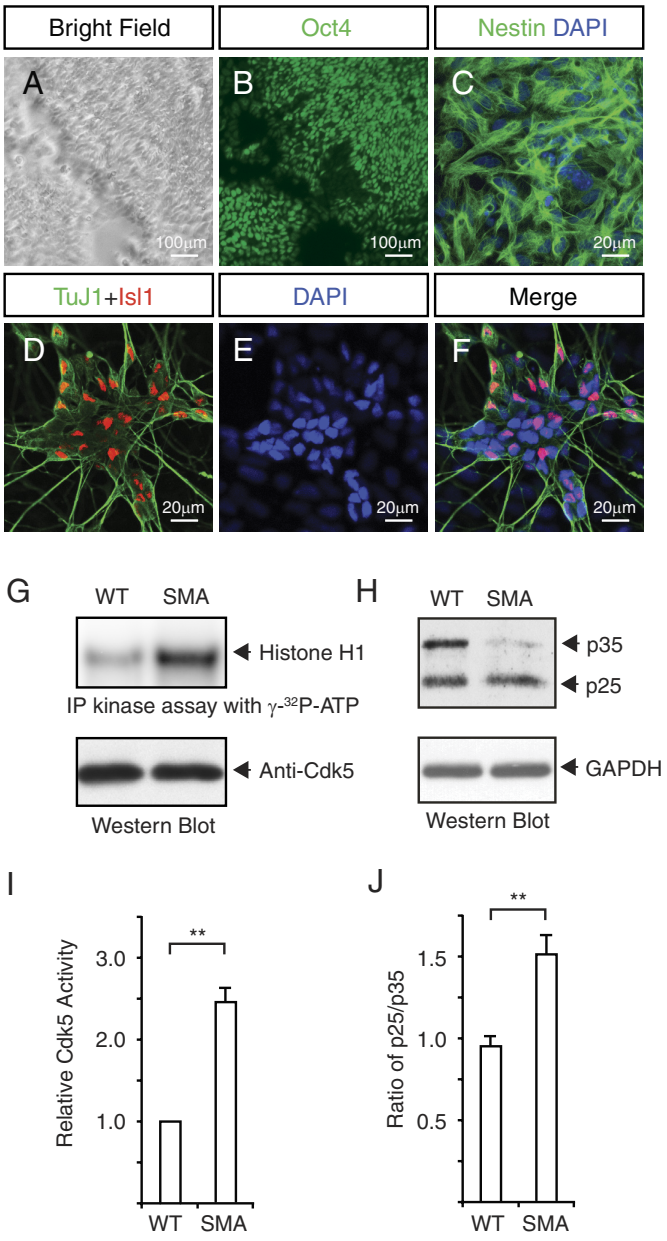

Fig. 3. Upregulation of Cdk5 activity and p25 level are conserved in human iPSC models of SMA. (*A*–*F*) Human iPSCs and iPSC-derived motor neurons serve as a model for studying SMA. Brightfield microscopy (*A*) and immunofluorescence staining (*B*–*F*) identify iPSCs (*A* and *B*) generated from SMA patient skin fibroblasts expressing the pluripotency marker Oct4 (green in *B*) and iPSC-derived neural progenitors expressing Nestin (green in *C*). After 6 wk in culture, human iPSC-derived motor neurons (*D*–*F*) express both neuronal marker TuJ1 (green in *D* and *F*) and motor neuron marker Isl1 (red in *D* and *F*). Cell nuclei were stained with DAPI (blue in *E* and *F*). (*G*–*J*) Endogenous Cdk5 kinase activity and the conversion of p35 to p25 are increased in human SMA iPSC-derived motor neurons. Cdk5 was immunoprecipitated from WT and SMA human iPSC-derived motor neurons after 6 wk in culture. Kinase activity (*G*) was measured by its phosphorylation of Histone H1 with ^{32}P-γ-ATP, shown by autoradiography in (*G*). The level of Cdk5 in each kinase assay reaction was monitored by Western blot. Kinase activities were quantified (*I*) using a phosphor imager. The ratio of p25 to p35 was measured by Western blot analysis (*H*) and quantified by densitometry (*J*) using GAPDH as equal loading control. Images are representative from four experiments, and data are mean ± SEM. $^{**}P < 0.01$, paired *t* test for (*I*) and unpaired *t* test for (*J*).

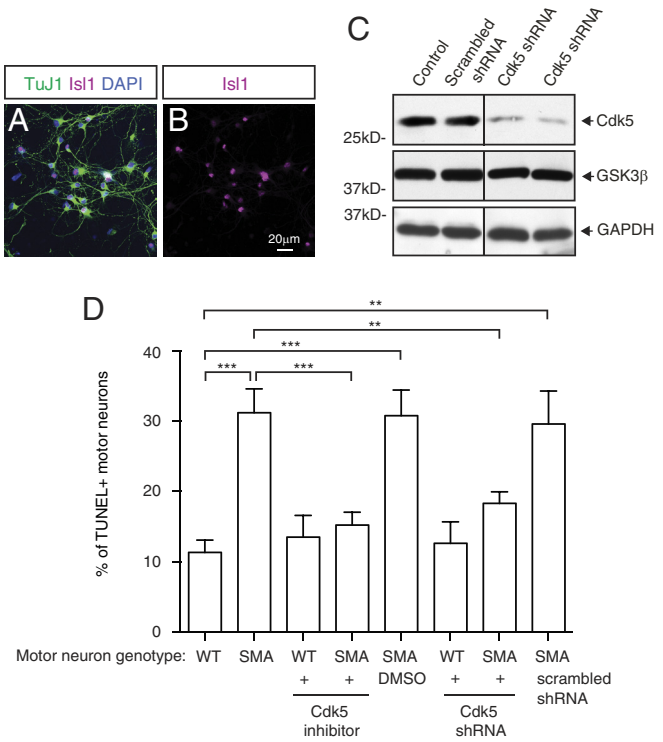

Fig. 4. Mitigating aberrant Cdk5 activation ameliorates the degeneration of motor neurons from SMA mice. (*A* and *B*) Primary spinal motor neurons from SMA mice cultured 6 days in vitro (6DIV) were stained by antibodies recognizing motor neuron marker Isl1 (magenta in *A* and *B*) and pan-neuronal marker TuJ1 (green in *A*). DAPI nuclear staining marks all cells in the culture. (*C*) Western blot analysis of Cdk5 knockdown in motor neurons treated with shRNA. Lentivirus-mediated shRNA targeting *Cdk5*, but not the scrambled control shRNA, can effectively knockdown the expression of Cdk5, but not GSK3β, in primary mouse spinal motor neurons. Motor neurons were infected with lentivirus on 4DIV and cultured for another 3 d before Western blot analysis. Two examples of Cdk5 shRNA knockdown were shown, with the expression of GAPDH as loading control. (*D*) Quantification of TUNEL+ degenerating motor neurons from WT and SMA mice. Inhibition of Cdk5 activity by applying 300 nM Cdk5 inhibitor BML259 or lentiviral shRNA to knockdown *Cdk5* in cultured motor neurons at 3DIV significantly reduced the degeneration of SMA motor neurons assayed on 6DIV. Data are eight sets from four independent experiments and are mean ± SEM. $^{**}P < 0.01$ and $^{***}P < 0.001$, Student's *t* test.

The reduced excitatory synapse formation on SMA motor neurons may change their functions. So we compared functional properties of motor neurons in WT, *SMA*, *SMA;p35*$^{-/-}$, and *p35*$^{-/-}$ mice using electrophysiological recordings. Whole-cell patch-clamp recording of WT, *SMA*, *SMA;p35*$^{-/-}$, and *p35*$^{-/-}$ mouse spinal cord tissue slices showed that motor neurons from all four genotypes were undistinguishable in whole cell input resistance, and action potential (AP) characteristics including AP duration, and AP rates of rise and fall (*SI Appendix*, Table S1). However, SMA motor neurons showed hyperexcitability in both their intrinsic currents and their firing behavior. The persistent inward current (PIC), a depolarizing current intrinsic to all neurons that sets the level of neuronal excitability, was significantly larger in SMA motor neurons, and was rescued to WT levels by genetic knockout of *p35*$^{-/-}$ in *SMA;p35*$^{-/-}$ mice (Fig. 6*G* and *SI Appendix*, Table S1). In addition, motor neuron firing behavior showed similar changes, with SMA motor neurons displaying a hyperpolarized threshold voltage, which was significantly restored in *SMA;p35*$^{-/-}$ motor neurons (Fig. 6*H* and *SI Appendix*, Table S1). Previous studies hypothesize that impairment of sensory-motor connectivity in SMA mice may lead to changes in motor neuron excitability and degeneration (20). The hyperexcitability of SMA motor neurons we observed in this study, including changes in the PIC and AP threshold voltage, supports this possibility. Our finding that hyperexcitability associated with SMA motor neurons could be reduced by genetic knockout of *p35* establishes a critical role for Cdk5 aberrant activation in motor neuron defects and SMA pathogenesis.

In addition to central excitatory synapse loss, another early and key pathogenic characteristic of SMA disease is compromised innervation of the NMJ by motor axons (18, 19, 69–71). In SMA mouse models, NMJ denervation was found in many muscles including the flexor digitorum brevis (FDB) controlling the second digit (FDB-2) (18, 19, 69, 70). Therefore, we examined NMJ innervation on FDB-2 in WT, SMA, *SMA;p35*$^{-/-}$, and *p35*$^{-/-}$ mice. We stained NMJ with anti-neurofilament and anti-synaptic vesicle 2 (SV2) antibodies to mark presynaptic structures, and α-bungarotoxin (BTX) to label postsynaptic acetylcholine receptors (AChRs) (Fig. 7 *A*–*D*). NMJs on FDB-2 were fully innervated in WT and *p35*$^{-/-}$ mice but showed significantly increased denervation or partial innervation in SMA mice (Fig. 7 *B* and *E*). Importantly, FDB-2 NMJ innervation in *SMA;p35*$^{-/-}$ mice was restored back to WT level, indicating that genetic knockout of *p35* rescues NMJ defects in SMA mice (Fig. 7 *A*–*E*).

NMJ denervation and central excitatory synapse loss have been suggested to contribute to motor neuron degeneration in SMA disease (18–21). To examine motor neuron degeneration in SMA mice, we stained lumbar level spinal cord sections with antibodies recognizing motor neuron marker Isl1. SMA mice showed dramatic reduction of motor neurons compared to WT mice, reflecting motor neuron degeneration in SMA (Fig. 7 *F*–*J*). Importantly, the number of motor neurons in *SMA;p35*$^{-/-}$ compound mutant mice was significantly restored, suggesting a beneficial effect of *p35* knockout on motor neuron degeneration in SMA pathogenesis (Fig. 7 *F*, *H*, and *J*). The survival life span of *SMA;p35*$^{-/-}$ double mutant mice was not improved, similar to results in other SMA genetic rescue studies (56, 72). This is likely because of the defects in cardiovascular and other systems in SMA mice (73–78) that cannot be rescued by genetic removal of *p35*, as p35 is predominantly expressed in neurons (49, 50). Taken together, these results suggest that genetic knockout of *p35* reduces motor neuron degeneration in SMA mice.

Inhibition of Cdk5 Signaling Reduces Human SMA iPSC Motor Neuron Degeneration. Attenuating up-regulated Cdk5 activity in SMA mice eases motor neuron degeneration. If similar improvements can be achieved in motor neurons from human SMA patients, it will suggest a potential therapeutic strategy. To test this possibility, we treated SMA or control human iPSC-derived motor neurons with Cdk5 inhibitor BML259 or calpain inhibitor Calpeptin (79–82), and examined motor neuron degeneration. Treatment with Cdk5 inhibitor or calpain inhibitor alleviates the degeneration of Isl1-positive motor neurons, while the application of DMSO vehicle as control had no effect (Fig. 8 *A*–*M*). Consistently, inhibition of Cdk5 signaling significantly reduced SMA iPSC motor neuron degeneration measured by staining with a different motor neuron marker ChAT or Terminal Transferase dUTP Nick End Labeling (TUNEL) assay (*SI Appendix*, Fig. S2 *A* and *B*). In addition, pharmacological inhibition of the Cdk5 signaling pathway showed similar beneficial effects on nonintegrating SMA iPSC-derived motor neurons (*SI Appendix*, Fig. S1*C*), indicating that these positive effects are not limited to specific human iPSC lines. Altogether, our findings suggest that inhibiting Cdk5 hyperactivation may represent a new strategy to alleviate SMA motor neuron degeneration in patients.

Discussion

Using mouse models and human iPSC models of SMA, we reveal that Cdk5 activity is significantly increased in SMA pathogenesis

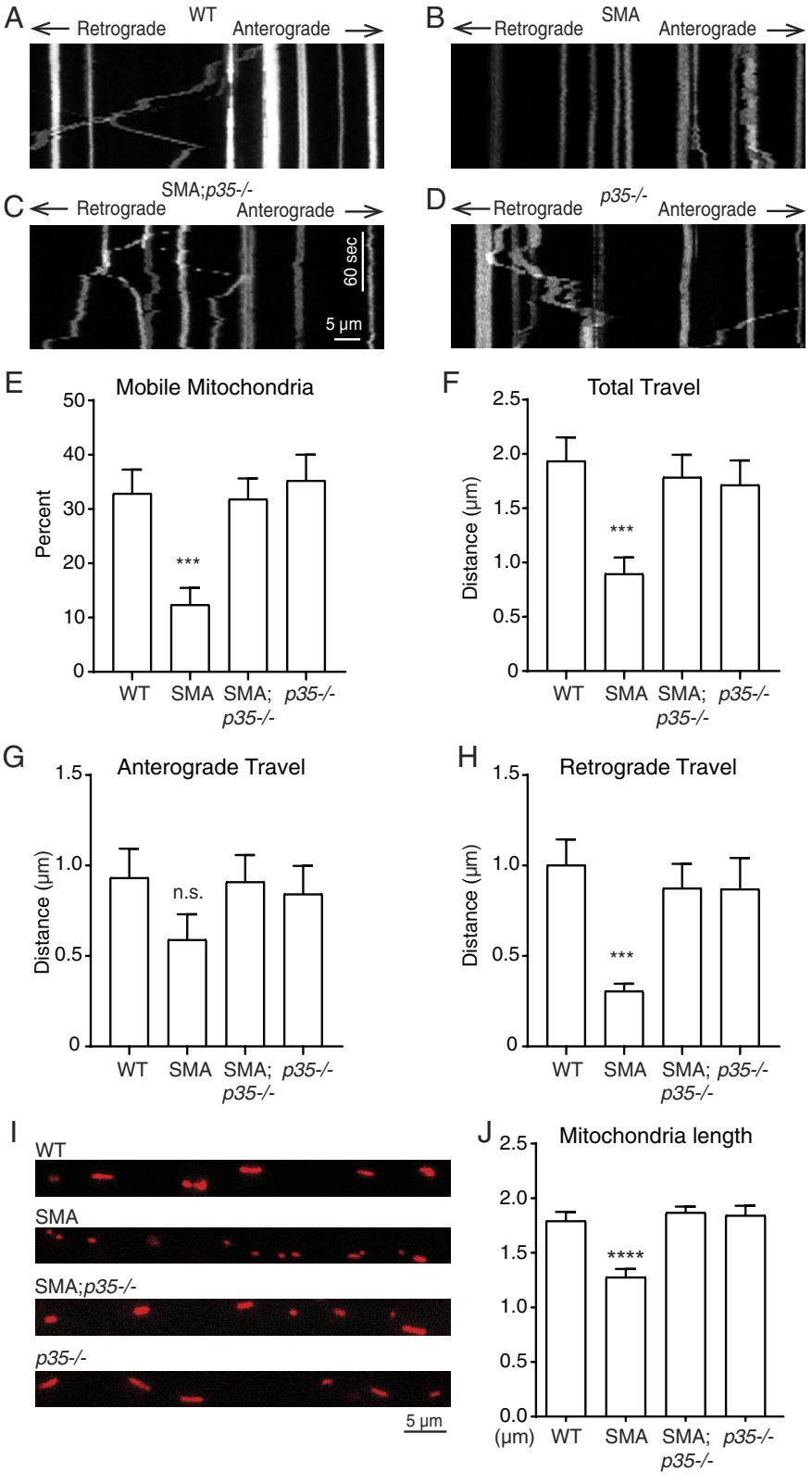

Fig. 5. Genetic knockout of *p35* rescues mitochondrial defects in SMA mouse motor neurons. (*A–D*) Representative kymographs of mitochondrial axon transport in WT, SMA, SMA;$p35^{-/-}$, and $p35^{-/-}$mice primary motor neurons. (*E–H*) Quantification of mitochondrial transport. The percentage of mobile mitochondria that travel more than 1 µm per minute (*E*) and the average total travel distance of all tracked mitochondria (*F*) are significantly reduced in SMA motor neurons and rescued to the WT level by genetic knockout of *p35* in SMA mice. The average total anterograde travel distance of all analyzed mitochondria is not changed in SMA motor neurons, while the retrograde travel distance is significantly reduced (*H*), which is restored to the WT level by the knockout of *p35* in SMA motor neurons. Data in *E–H* are quantification of mitochondria in 27 neurons from each genotype (WT: n = 259; SMA: n = 236; SMA;$p35^{-/-}$: n = 273; $p35^{-/-}$: n = 181 mitochondria) and are mean ± SEM. ***$P < 0.001$, one-way ANOVA with Tukey HSD post hoc analysis. (*I* and *J*) Genetic knockout of *p35* rescues mitochondrial fragmentation in SMA motor neurons. (*I*) Representative images for measuring mitochondrial length in WT, SMA, SMA;$p35^{-/-}$, and $p35^{-/-}$mouse motor neurons transfected with mito-dsRed and quantified using confocal live imaging. (*J*) Mitochondrial length in spinal motor neurons from SMA mice is significantly shorter, which is rescued to the WT level by the knockout of *p35* in SMA mice. Data in *J* are quantification of mitochondria in 27 neurons from each genotype (WT: n = 211; SMA: n = 228; SMA;$p35^{-/-}$: n = 187; $p35^{-/-}$: n = 122 mitochondria), and are mean ± SEM. ****$P < 0.0001$, one-way ANOVA with Tukey HSD post hoc analysis.

before the onset of disease symptoms. Genetic reduction of Cdk5 activation in SMA mice rescues mitochondrial defects and other diverse SMA disease phenotypes in vivo. Notably, inhibition of Cdk5 signaling ameliorates the degeneration of motor neurons derived from human SMA iPSCs and SMA mouse models, providing insights into the pathogenic mechanism and a potential therapeutic strategy for SMA.

A Positive Feedback Loop Formed by Aberrant Cdk5 Activation and Mitochondrial Defects Leading to Motor Neuron Degeneration in SMA. One important finding from this study is that genetic knockout of *p35* rescues mitochondrial defects in motor neurons affected by SMA, revealing a critical signaling mechanism underlying the mitochondrial phenotypes in SMA motor neurons we identified (22). Mitochondria play a central

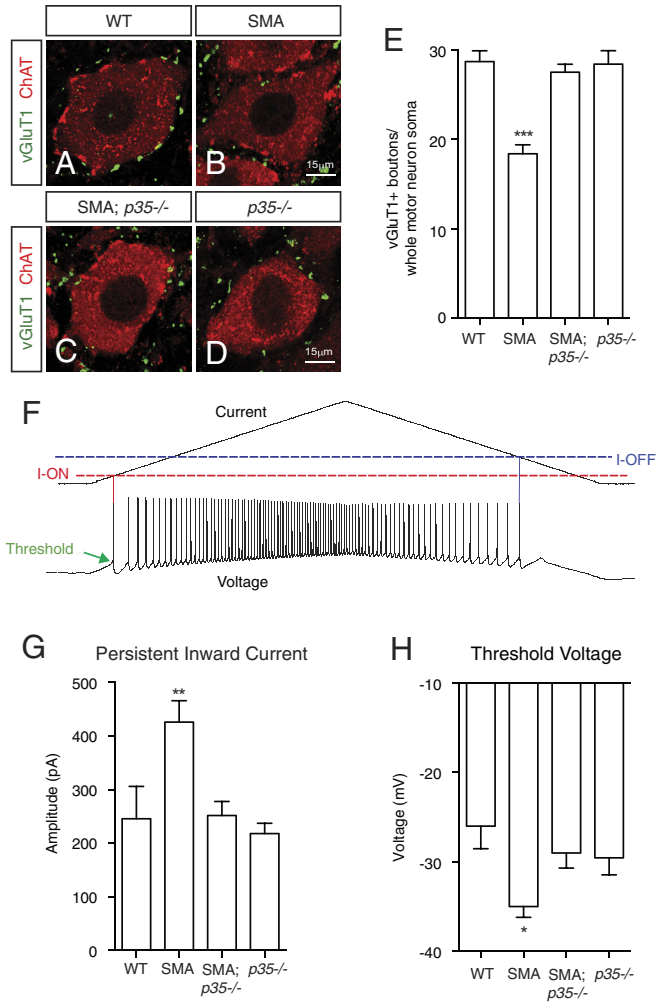

Fig. 6. Genetic knockout of *p35* alleviates synaptic defects and hyperexcitability in SMA mouse motor neurons. (*A–E*) Excitatory glutamatergic synapse loss on SMA spinal cord motor neurons can be rescued by *p35* knockout. Colocalization of the glutamatergic synapse marker vGluT1 (green in *A–D*) with the motor neuron marker ChAT (red in *A–D*) by immunostaining shows that excitatory synaptic boutons on motor neurons are significantly reduced in SMA mice and rescued to the WT level by genetic knockout of *p35* in SMA mice (*E*). Data in *E* are quantified from motor neurons of three to four mice from each genotype (WT: n = 42; SMA: n = 51; *SMA;p35*$^{-/-}$: n = 54; *p35*$^{-/-}$: n = 34 motor neurons) and are mean ± SEM. ***$P < 0.001$, one-way ANOVA with Tukey HSD post hoc analysis. (*F–H*) SMA spinal motor neuron hyperexcitability can be reduced by genetic knockout of *p35*. Example plot of a firing motor neuron recorded during depolarizing current ramps (*F*). Threshold voltage (green), I-ON (red), and I-OFF (blue) were measured as shown. (*G* and *H*). Whole-cell patch-clamp electrophysiological recording of spinal motor neurons from P7-9 SMA mice showed that the amplitude (*G*) of PIC, which indicates the level of cellular excitability, was significantly increased in SMA motor neurons, and rescued in *SMA;p35*$^{-/-}$ mice. Threshold voltage (*H*) of AP firing is significantly more hyperpolarized in SMA motor neurons but not in motor neurons from *SMA;p35*$^{-/-}$ mice. Quantifications are from four mice of each genotype and are mean ± SEM. *$P < 0.05$ and **$P < 0.01$, one-way ANOVA with Tukey HSD post hoc analysis.

role in generating energy and buffering Ca^{2+}. In highly polarized motor neurons, healthy mitochondria are dynamically transported to regions that need more energy and Ca^{2+} buffering (83–85). Mitochondrial functions are closely affected by its size and morphology. Elongated mitochondria have higher density of cristae with better efficiency in ATP production; whereas short and fragmented mitochondria, as seen in SMA motor neurons, are more likely to have compromised Ca^{2+} buffering capacity and low efficiency in ATP production (22, 68). The hyperexcitability of SMA motor neurons, shown by our electrophysiology recording (Fig. 6 *F–H* and *SI Appendix*, Table S1), leads to their particularly high demand for energy supply and Ca^{2+} buffering. However, mitochondrial transport and fragmentation defects in SMA motor neurons reduce their capacity for energy production and Ca^{2+} buffering, further exacerbating the abnormal increase of intracellular Ca^{2+} and energy shortage created by hyperexcitability. Consequently, increased Ca^{2+} activation of calpain and up-regulated calpain conversion of p35 to p25 further activate Cdk5, and Cdk5 hyperphosphorylation of targets that cause mitochondrial dysfunction leads to more severe energy shortage and disrupted Ca^{2+} buffering. Activation of this positive feedback loop in SMA pathogenesis eventually turns motor neuron hyperexcitability to excitotoxicity and degeneration. Our findings highlight an aberrant Cdk5 activation-centered mechanism that contributes to SMA pathogenesis.

The Presymptomatic Upregulation of Cdk5 Activity in SMA. The activation of Cdk5 we found in SMA is different from other neurodegenerative disorders. First, in SMA mouse models, Cdk5 activity is up-regulated before the onset of disease phenotypes, suggesting that increased Cdk5 activity may be a cause, rather than a consequence, of SMA pathogenesis. By contrast, previous studies of the hyperactivation of Cdk5 in Alzheimer's disease and ALS were conducted on samples that already displayed disease symptoms (43, 44). In SMA mouse models we observed significant upregulation of Cdk5 activity as early as postnatal day 3 (P3), when SMA and non-disease littermate control mice are indistinguishable at the behavioral and cellular levels, suggesting that aberrant Cdk5 activation may be part of the mechanisms that initiate SMA disease. Thus, mitigating Cdk5 activity may represent a strategy to alleviate SMA pathology through early intervention. Second, the upstream cause of Cdk5 hyperactivation in SMA, a pediatric neuromuscular disorder, is likely different from that in aging-associated neurodegeneration. Both genetic mutations and age-dependent nongenetic risk factors contribute to the pathogenesis of Alzheimer's disease and ALS. By contrast, SMA is a monogenic disorder caused by mutations in the *SMN1* gene, leading to reduced SMN protein level. SMN has been implicated in regulating snRNP biogenesis and pre-mRNA splicing (12, 15, 86). RNA splicing and expression defects in calcium channel and other mechanisms regulating calcium homeostasis have been revealed by RNA-Seq analysis of motor neurons affected by SMA (16, 87–89). These defects provide a potential link that connects reduced SMN protein level, through disrupting calcium homeostasis and increased Ca^{2+}-dependent calpain cleavage of p35 to p25, with aberrant Cdk5 activation in SMA.

Cdk5 Targets in SMA Pathogenesis. What downstream targets of Cdk5 could lead to SMA disease phenotypes? MDAS domain transcription factor myocyte enhancer factor 2 (MEF2), dynein-interacting nuclear distribution protein nudE-like 1 (Ndel1), mitochondrial fission regulator dynein-related protein 1 (Drp1), and microtubule-associated protein tau, which can be phosphorylated by Cdk5 (30, 46, 56, 66, 90, 91), are likely critical contributors. We have found that microtubule-associating protein tau phosphorylation by Cdk5 was dramatically increased in SMA without causing protein fibrillary tangles or aggregates (56), which is different from neurodegenerative disorders associated with up-regulated Cdk5 activity and protein aggregation (43, 44). In SMA, increased Cdk5 phosphorylation of tau may contribute to disease pathogenesis by disrupting axonal transport and tau interaction with prosurvival factors, and by causing excitotoxicity. Increased phosphorylation of tau impairs microtubule assembly in axons and compromises microtubule-dependent protein and organelle transport (92, 93), which may be particularly exacerbated in

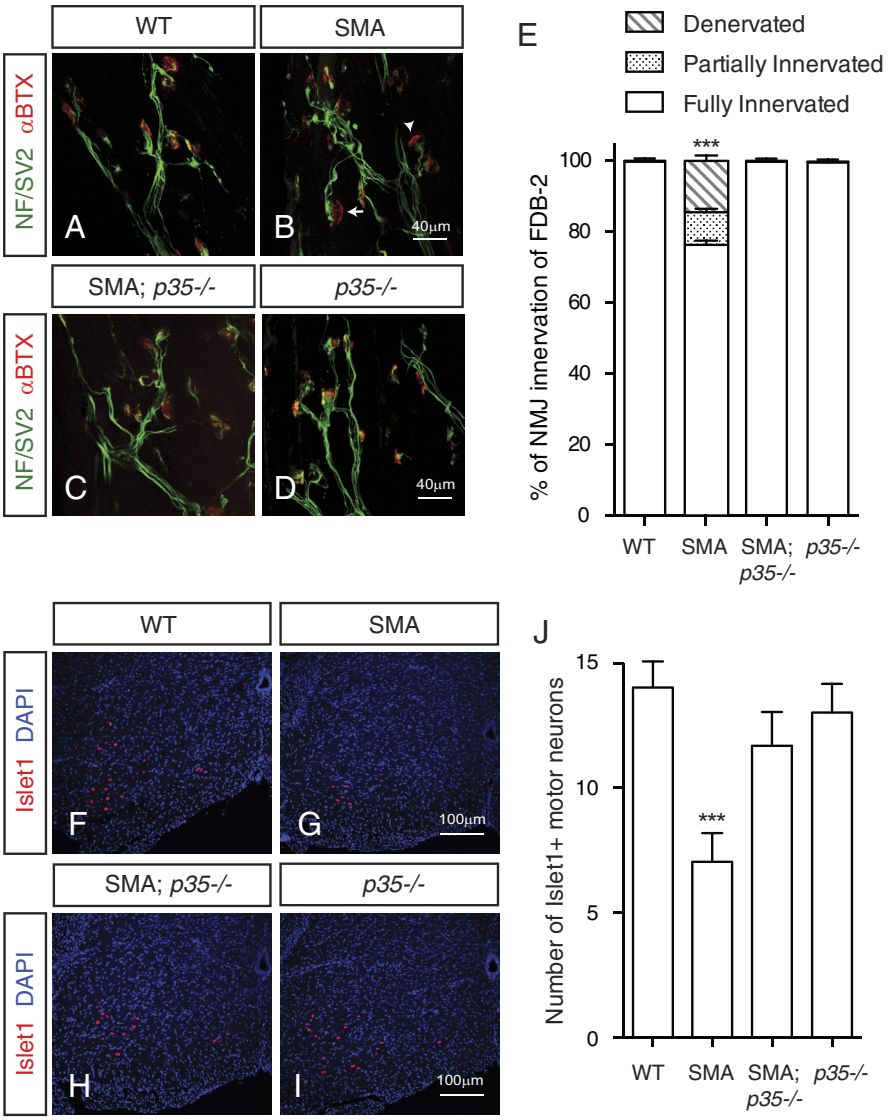

Fig. 7. Genetic knockout of *p35* rescues NMJ defects and motor neuron degeneration in SMA mice. (*A–E*) Motor neuron axon denervation at NMJs in SMA mice can be rescued by genetic knockout of *p35*. Colocalization of presynaptic nerve terminals marked by immunostaining with anti-neurofilament (NF) and anti-SV2 antibodies (green in *A–D*) with postsynaptic AChRs labeled by α-bungarotoxin (αBTX) (red in *A–D*) shows increased denervation (arrowheads) and partial innervation (arrow) of NMJs on the FDB-2 muscle of SMA mice. The NMJ innervation defect is rescued to the WT level in *SMA;p35*$^{-/-}$ mice. Quantification in *E* is from over 120 NMJs on the FDB-2 muscle from each mouse. Five mice for each genotype were used. Denervated, partially innervated, and fully innervated NMJs were analyzed separately. Results are mean ± SEM. ***$P < 0.001$, one-way ANOVA with Tukey HSD post hoc analysis. (*F–J*) Motor neuron degeneration in SMA mice is reduced by *p35* knockout. Lumbar level spinal cord sections of P9 SMA mice show a near 40% reduction of Islet1-positive (red in *F–I*) motor neurons compared to WT littermates. Genetic knockout of *p35* reduces motor neuron degeneration in *SMA;p35*$^{-/-}$ mice (*J*). Data in *J* are from four to five mice of each genotype in four independent experiments (WT: n = 130; SMA: n = 144; *SMA;p35*$^{-/-}$: n = 162; *p35*$^{-/-}$: n = 129 sections) and are mean ± SEM. ***$P < 0.001$, one-way ANOVA with Tukey HSD post hoc analysis.

spinal motor neurons that have long axons, contributing to the selective vulnerability of motor neurons in SMA. In addition, increased tau phosphorylation in SMA may disrupt complexes formed by tau-binding partners, including phosphatidylinositol 3-kinase (PI3K) and Src family kinases that are critical for neuronal survival (94–96). Moreover, tau has been shown to be required for targeting Src family kinase Fyn to phosphorylate NR2B and prevent NMDA receptor-mediated excitotoxicity (97). Increased phosphorylation of tau could disrupt the balance between excitatory and inhibitory synaptic inputs on motor neurons, leading to excitotoxicity in SMA. Regarding MEF2, it regulates neuronal survival, neurite outgrowth, and synapse elimination (90, 98–101), which are very relevant to the central excitatory synapse loss phenotype and NMJ denervation observed in SMA. The temporal expression of MEF2 peaks at the early postnatal stage when synapse elimination and motor neuron target innervation is most active. One critical MEF2 target gene involved in regulating axonal morphogenesis, synaptic elimination and neuronal survival is *brain-derived neurotrophic factor* (*bdnf*) (98, 100, 102). When we measured the expression of *bdnf* in SMA mouse spinal cords using RT-qPCR, *bdnf* expression showed a significant decrease in spinal cords from SMA mice compared to control littermates (*SI Appendix*, Fig. S2*C*), supporting a role for the dysregulation of MEF2 target gene expression in SMA pathogenesis. In addition, MEF2 has been shown to be physically present in mitochondria and function as a mitochondrial transcription factor to directly regulate the expression of mitochondrial complex I component *ND6* gene encoded by mitochondrial DNA (103). Complex I is one of the main sites of mitochondrial reactive oxygen species production, defects in complex I cause mitochondrial oxidative stress (104, 105). Thus, the MEF2 regulation of mitochondrial DNA-encoded gene expression may provide a direct link between aberrant Cdk5 activation and mitochondrial defects in SMA. Besides MEF2, Cdk5 target Ndel1 and Drp1 are likely involved in regulating defective mitochondrial transport and fragmentation, respectively. Cdk5 phosphorylates Ndel1 in the Lis1/Ndel1/dynein complex to activate dynein-dependent retrograde axonal transport (37), while hyperphosphorylation of Ndel1 by aberrant Cdk5 activation disrupts retrograde transport (30). In addition, Cdk5 phosphorylation of mitochondrial fission regulator Drp1 has been linked to increased mitochondrial fragmentation (66). These mechanisms may lead to mitochondrial retrograde transport and fragmentation defects that we observed in SMA motor neurons (Fig. 5). Altogether, phosphorylation of diverse targets by aberrantly activated Cdk5 may contribute to SMA pathogenesis through multiple pathways.

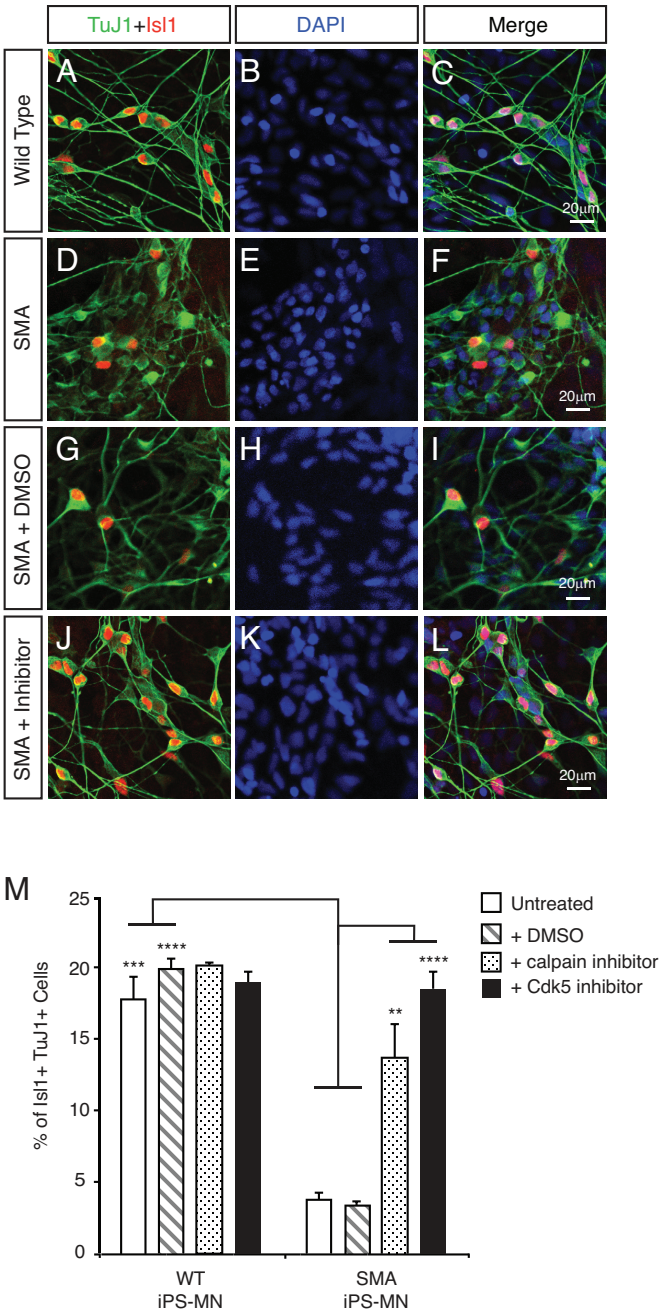

Fig. 8. Inhibition of the Cdk5 signaling pathway decreases the degeneration of human SMA iPSC-derived motor neurons. (*A–L*) Immunostaining of human iPSC-derived motor neurons with antibodies recognizing neuronal marker TuJ1 (green in *A–L*), motor neuron marker Isl1 (red in *A–L*), and nucleus marker DAPI (blue in *A–L*). Treatment of human SMA iPSC motor neurons from weeks 3 to 6 in culture with a calpain inhibitor significantly increases the number of Isl1-positive motor neurons, while DMSO vehicle control has no effect. (*M*) Quantification of TuJ1 and Isl1-positive motor neurons as a percentage of all DAPI-positive cells in a human iPSC model of SMA treated with inhibitors of Cdk5 signaling. Application of 300 nM Cdk5 inhibitor BML259 or 10 μM calpain inhibitors Calpeptin from week 3 to week 6 in human SMA iPSC culture significantly reduces the degeneration of motor neurons. Data are from four independent experiments and are mean ± SEM. $^{**}P < 0.01$, $^{***}P < 0.001$, and $^{****}P < 0.0001$, Student's *t* test.

Implications for SMA Treatment. An important observation in our study was that the upregulation of Cdk5 activity and the increased conversion of p35 to p25 in SMA disease are conserved between mice and humans. Our finding that inhibition of Cdk5 and calpain can attenuate motor neuron degeneration in human SMA iPSC-derived motor neurons (Fig. 8) suggests that inhibiting the Cdk5 signaling pathway may be used to benefit human patients.

It is worth noting that genetic knockout of *p35* in SMA mice significantly rescued disease phenotypes, including mitochondrial defects, NMJ denervation and spinal motor neuron degeneration. This is likely due to the functional importance of Cdk5 signaling in spinal motor neurons and neural muscular junction (33, 35, 55). While the functional redundancy between p35 and Cdk5 activator p39, and the relatively high expression level of p39 in mouse spinal cord (49) leads to the maintenance of some essential basal Cdk5 activities in the SMA;$p35^{-/-}$ mice. Existing strategies for treating SMA are mostly based on increasing full-length functional SMN protein (24–26, 106), which has significant limitations (27). As such, one important focus of future studies is to test the potential use of this strategy in SMA animal models and humans to reverse or delay the onset of SMA symptoms in vivo. Inhibition of the Cdk5 signaling pathway may be used in combination with other treatments to improve motor neuron health and survival. Inhibitors of the Cdk5 pathway have been developed for neurodegeneration, cancer, and neuronal injury (29, 107–110), which may be repurposed for treating SMA. Roscovitine has also been proposed to improve SMA motor neuron function by modifying calcium channels and calcium homeostasis (89). A short peptide fragment of p35 was identified to specifically inhibit the aberrant activation of Cdk5 without affecting its normal physiological functions (110–112). Expression of this Cdk5 inhibitory peptide in mice reduces neurodegeneration in vivo without inhibiting endogenous or transfected p35/Cdk5 activity, or other cyclin-dependent kinases (110–112). Therefore, similar inhibitory peptides, or inhibitors that specifically disrupt the interaction between Cdk5 and its targets in SMA, can be developed to alleviate motor neuron disease symptoms. Taken together, mitigating aberrant Cdk5 activation represents a strategy to treat and benefit SMA patients. Further exploration of the Cdk5-related mechanisms will have implications for understanding the pathogenesis and therapy of SMA and other neurodegenerative disorders.

Materials and Methods

Mice. The Δ7 SMA mice (*Smn*$^{-/-}$;*SMN2*$^{tg/tg}$;*SMNΔ7*$^{tg/tg}$, or Jackson Lab #005025) (57) and the Hung-Li SMA mice (*Smn*$^{-/-}$;*SMN2Hung*$^{tg/-}$, or Jackson Lab # 005058) (58) were obtained from Jackson Laboratory. Pups were genotyped by PCR with genomic DNA extracted from tail samples (57, 58). The *p35* knockout mice were generated and provided by Li-Huei Tsai's laboratory and genotyped as reported (65). Both male and female mice were used. ARRIVE guidelines were followed for the animal experiments. Investigators were blinded to the treatment groups.

Human SMA iPSC and Mouse Motor Neuron Culture. Human iPSCs were generated and differentiated as previously described (61, 62). Briefly, primary fibroblasts were isolated from deidentified type I SMA patients and their unaffected relatives, infected with lentiviral constructs expressing *OCT4*, *SOX2*, *NANOG*, and *LIN28* (61) or episomally expressed reprogramming plasmids (62) to generate iPSCs. Retinoic acid, sonic hedgehog, cAMP, ascorbic acid, BDNF, and glial cell line-derived neurotrophic factor (GDNF) were used to induce iPSC spheres to differentiate into motor neurons. Primary neurons from mouse spinal cords were cultured in Neurobasal (Life Technologies) supplemented with B27 (Life Technologies) as described (22, 56). Briefly, spinal cords from E12.5 mouse embryos were dissected out and dissociated with 0.25% trypsin. After enriching motor neurons with OptiPrep density gradient centrifugation and BSA cushion, cells were seeded on glass coverslips coated with 20 μg/mL Poly-L-Lysine (PLL) (Sigma) and 8 μg/mL Laminin (Sigma) and grown in the presence of 50 μg/mL BDNF, 50 μg/mL CNTF and 25 μg/mL GDNF (PeproTech). Cell death was detected by the in situ cell death detection TMR red TUNEL kit. Cdk5 inhibitor BML259 (300 nM) (Cayman Chemical) and calpain inhibitor Calpeptin (10 μM) (Tocris Bioscience) were applied from weeks 3 to 6 into iPSC motor neuron medium to inhibit Cdk5 signaling.

In Vitro Cdk5 Kinase Assay. Endogenous Cdk5 kinase in spinal cord lysates was immunoprecipitated with anti-Cdk5 antibodies [C17 monoclonal (39) or Cell Signaling #2506]. The Cdk5 kinase immunoprecipitation complexes were washed and suspended in kinase buffer containing 50 mM Hepes (pH7.4), 5 mM $MnCl_2$, 5 mM $MgCl_2$, and 2 mM DTT and incubated with 2 μg purified Histone H1 (Sigma) in the presence of 1 μM ATP and 10 μM γ-^{32}P-ATP at 30 °C for 15 min. Samples were then denatured in sodium dodecyl sulfate (SDS) sample buffer, separated on polyacrylamide gel electrophoresis (SDS-PAGE), and subjected to autoradiography, scintillation counting, and phosphor imager quantification (59). Relative endogenous Cdk5 activity was calculated by dividing the Cdk5 kinase activity of each SMA spinal cord sample with the kinase activity of its paired WT sample.

Confocal Live Imaging and Data Analysis of Mitochondria Transport and Length. Time-lapse live imaging by confocal microscope was used to measure axonal mitochondrial transport and length. After culturing for 5 to 7 d, primary mouse spinal motor neurons were transfected with mitochondria targeting sequence-tagged DsRed (mito-DsRed). 48 h after transfection, images were acquired using a Zeiss LSM 700 confocal microscope equipped with a 63X/NA 1.15 water LD C-Apochromat objective lens and a temperature (37 °C) and CO_2 (5%) controlled stage. Images were captured every 2 s for a period of 2 min using Zen software. The 561 nm laser intensity was set at 0.2 mW to minimize damage, and pinholes were opened maximally to allow the entire thickness of the axon to be imaged. Axon fragments of 50 to 100 μm in length located at least 50 μm away from the cell body were selected for analysis. A custom-made Image J plug-ins was used to generate kymographs and analyze mitochondria motility and length (22).

Electrophysiological Recording. Mice at P7–8 were deeply anesthetized with isofluorane, decapitated, and eviscerated. The lower thoracic to upper lumbar spinal cord was removed and embedded in 2.5% w/v agar. Using the Leica 1000 vibratome, 350-μm transverse slices were made as described previously (113). During spinal cord isolation and slicing, the spinal cord was immersed in 1 to 4 °C high osmolarity dissecting solution containing (in mM) sucrose 234.0, KCl 2.5, $CaCl_2$ $2H_2O$ 0.1, $MgSO_4$ $7H_2O$ 4.0, HEPES 15.0, glucose 11.0, and Na_2PO_4 1.0. After cutting, the slices were incubated for >1 h at 30 °C in incubating solution containing (in mM) NaCl 126.0, KCl 2.5, $CaCl_2$ $2H_2O$ 2.0, $MgCl_2$ $6H_2O$ 2.0, $NaHCO_3$ 26.0, and glucose 10.0. Whole-cell patch clamp was performed at room temperature on motor neurons using 2 to 5 MΩ glass electrodes positioned using a Sutter Instrument MP-285 micromanipulator. Slices were perfused with a modified Ringer's solution containing (in mM): 111 NaCl, 3.09 KCl, 25.0 $NaHCO_3$, 1.10 KH_2PO_4, 1.26 $MgSO_4$, 2.52 $CaCl_2$, and 11.1 glucose. All solutions were continuously oxygenated with 95% O_2 and 5% CO_2. Recordings were performed in current and voltage clamp modes as described (113) using the MultiClamp 700B amplifier (Molecular Devices, Burlingame, CA). Patch electrodes contained (in mM) 138 K-gluconate, 10 HEPES, 5 ATP-Mg, and 0.3 GTP-Li (all from Sigma, St. Louis, MO). In voltage clamp mode, neurons were subjected to slow, depolarizing voltage ramps to measure the PIC bringing the cell from −90 mV holding potential to 0 mV in 8 s, and then back to −90 mV in the following 8 s. In current clamp, neurons were subjected to depolarizing current ramps to measure I_{ON} (the current level at firing onset), I_{OFF} (the current level at cessation of firing), and the frequency–current relationship. The medial motor neuron pools could be easily visualized in the slice preparation using DIC optics, and electrodes were positioned above this area. Individual neurons were targeted based on large soma diameter (>20 μM long axis) and only neurons with an input resistance <100 MΩ, a resting potential <−50 mV, and a series resistance of <20 MΩ were included in this study. Neurons were eliminated from analysis if series resistance or resting potential varied more than 10 MΩ or 10 mV, respectively, throughout the recording period. Data were collected on WinFluor software (University of Strathclyde, Glasgow, Scotland) and analyzed using Spike2 software (Cambridge Electronic Design, Cambridge, England). Graphs and statistics were performed using Microsoft Excel and GraphPad Prism.

Lentiviral shRNA and Real-Time PCR. Lentivirus expressing shRNA for Cdk5 and scrambled control were purchased from Santa Cruz Biotechnologies. For real-time quantitative PCR assay, total RNA was extracted from the homogenized mouse spinal cord with the RNeasy kit (Qiagen) and treated with the RNase-Free DNase Set (Qiagen). For cDNA synthesis, 1 μg of total RNA was used for reverse transcription using the oligo(dT)-primer and SuperScript III kit (Invitrogen). Real-time PCR was performed using SYBR Green PCR Master Mix (Applied Biosystems) and measured with the Applied Biosystems 7500 Real-Time PCR System. Primers used for the RT-qPCR are as follows: *bdnf*: Forward (F) GATGCCGCAAACATGTCTATGA, Reverse (R) TAATACTGTCACACACGCTCAGCTC; *gapdh*: (F) CATGGCCTTCCGTGTTCCT, (R) TGATGTCATCATACTTGGCAGGTT; *actin*: (F) GCGAGCACAGCTTCTTTGC, (R) TCGTCATCCATGGCGAACT; and *tubulin*: (F) CGACAATGAAGCCCTCTACGAC, (R) ATGGTGGCAGACACAAGGTGGTTG.

Immunohistochemistry. SMA and WT mice were perfused with PBS and 4% PFA. Spinal cords were isolated and fixed overnight in freshly made 4% PFA. All samples were washed extensively with PBS and treated sequentially with 15% and 30% sucrose before embedding into OCT. Cryosections of 18 μm thick were then prepared with a Leica CM1950 cryostat. For immunostaining, tissue sections were first treated with 10 mM citric acid antigen retrieval solution (DAKO) at 98 °C for 20 min and then permeabilized in 0.25% Triton X-100 and blocked with 5% donkey serum and 5% goat serum in PBST buffer (PBS with 0.05% Tween-20). Samples were then incubated with primary antibodies overnight at 4 °C, washed with PBST, incubated with secondary antibodies, washed with PBST, mounted in Aqua-Mount (Fisher Scientific), and imaged with a Zeiss LSM510 confocal microscope. Primary antibodies used in this study are as follows: p35/p25 (1:500, Cell Signaling #2680 rabbit monoclonal), Isl1 (1:750, Developmental Studies Hybridoma Bank 40.2D6 mouse monoclonal), SV2 (1:10, Developmental Studies Hybridoma Bank mouse monoclonal), ChAT (1:100, Chemicon AB144P goat polyclonal), vGluT1 (1:500, Synaptic System 135303, rabbit polyclonal), neurofilament (1:100, Developmental Studies Hybridoma Bank 2H3 mouse monoclonal), α-bungarotoxin (1:1,000, Invitrogen, Alexa 594-conjugated), and TuJ1 (1:1,000, Covance MRB-435P rabbit polyclonal). Secondary antibodies are from Jackson ImmunoResearch and used at 1:500 dilution.

NMJs of mouse FDB muscles were stained as previously reported (56). Briefly, FDB muscles were isolated and teased into layers of 5 to 10 fibers thick to facilitate penetration of antibodies. Presynaptic nerve terminals were labeled with anti-neurofilament and anti-SV2 antibodies. AChRs were labeled by α-bungarotoxin. Z-stack images of fluorescently labeled NMJs were captured at sequential focal planes 1 μm apart using a Zeiss LSM 510 META confocal microscope. All confocal images were taken using the same imaging parameters, including laser intensities, amplification gains, and offsets. To study excitatory synapse formation on spinal motor neurons, lumbar spinal cord segments (L1–2) were dissected and processed for 80 μm-thick vibratome (Leica) sections. Motor neurons were labeled with anti-ChAT antibody and excitatory presynaptic terminals with anti-vGluT1. Glutamatergic synapses were identified as boutons opposed to membrane of motor neuron soma and proximal dendrites. The number of synapses from Z-stack images of the whole motor neuron soma was counted. Statistical significance was determined using one-way ANOVA analysis with Tukey honestly significant difference (HSD) post hoc analysis.

Western Blotting and Immunoprecipitation. Spinal cord samples or motor neurons were lysed in the buffer containing 200 mM NaCl, 0.4% Triton X-100, 0.7% CHAPS, 50 mM Tris pH8.0, 5 mM EDTA, and 5 mM DTT plus proteinase inhibitors to be used for Western blotting or immunoprecipitation. Samples were homogenized by a polytron handheld homogenizer (Kinematica) and quantified using the BCA Protein Assay Kit (Pierce). All proteins were separated with 10% SDS-PAGE and then transferred to PVDF membrane and incubated with indicated antibodies. Primary antibodies were diluted in TBS containing 0.05% Tween-20 and 5% bovine serum albumin as follows: Cdk5 (1:5, Li-Huei Tsai C-17 mouse monoclonal), p35/p25 (1:500, Cell Signaling #2680 rabbit monoclonal), GSK3b (1:500, Cell Signaling #12456 rabbit monoclonal), GAPDH (1:1,000, Santa Cruz Biotech SC-25778 rabbit polyclonal), and Histone H1 (1:500, Santa Cruz Biotech SC-8030 mouse monoclonal). Horseradish peroxidase (HRP)-conjugated secondary antibodies (1:10,000, Jackson ImmunoResearch) and Femto LUCENT plus HRP reagent kit (G Biosciences) were used for exposure and quantification.

Data, Materials, and Software Availability. All study data are included in the article and/or *SI Appendix*.

ACKNOWLEDGMENTS. We thank Dr. Christine J. DiDonato for providing some SMA mice for breeding initially and helping us with SMA mouse behavioral assays, Dr. L.-H.T. for providing the *p35* knockout mouse line and the anti-Cdk5 C-17 mouse monoclonal antibody, and Dr. Monal Patel and Dr. Markus E. Peter for providing the facilities to do some of the radioactive kinase assays. We thank Michael Kahl for critically reading the manuscript. We acknowledge Hehai

Wang and Ben Yang for their technical assistance with immunohistochemistry and Western blot analyses. Y.C.M. is supported by NIH grants R01NS094564, R21NS106307, and RF1AG077451 and grants from the Hartwell Foundation and Cure SMA. The research reported in this manuscript was made possible in part by the generous support of the Agape Foundation.

Author affiliations: [a]Department of Pediatrics, Northwestern University Feinberg School of Medicine, Chicago, IL 60611; [b]Stanley Manne Children's Research Institute, Ann and Robert H. Lurie Children's Hospital of Chicago, Chicago, IL 60611; [c]Department of Neuroscience, Northwestern University Feinberg School of Medicine, Chicago, IL 60611; [d]Department of Physical Medicine and Rehabilitation, Northwestern University Feinberg School of Medicine, Chicago, IL 60611; [e]Department of Physical Therapy and Human Movement Sciences, Northwestern University Feinberg School of Medicine, Chicago, IL 60611; [f]Department of Biomedical and Pharmaceutical Sciences, College of Pharmacy, George and Anne Ryan Institute for Neuroscience, University of Rhode Island, Kingston, RI 02881; [g]Department of Cell Biology, Neurobiology and Anatomy, Medical College of Wisconsin, Milwaukee, WI 53226; [h]Section of Neurobiology, Department of Biological Sciences, University of Southern California, Los Angeles, CA 90089; and [i]Department of Brain and Cognitive Sciences, Picower Institute for Learning and Memory, Massachusetts Institute of Technology, Cambridge, MA 02139

1. B. Wirth, M. Karakaya, M. J. Kye, N. Mendoza-Ferreira, Twenty-five years of spinal muscular atrophy research: From phenotype to genotype to therapy, and what comes next. *Annu. Rev. Genomics Hum. Genet.* **21**, 231–261 (2020).
2. A. H. Burghes, C. E. Beattie, Spinal muscular atrophy: Why do low levels of survival motor neuron protein make motor neurons sick? *Nat. Rev. Neurosci.* **10**, 597–609 (2009).
3. H. Chaytow, K. M. E. Faller, Y. T. Huang, T. H. Gillingwater, Spinal muscular atrophy: From approved therapies to future therapeutic targets for personalized medicine. *Cell Rep. Med.* **2**, 100346 (2021).
4. M. Van Alstyne, L. Pellizzoni, Advances in modeling and treating spinal muscular atrophy. *Curr. Opin. Neurol.* **29**, 549–556 (2016).
5. C. L. Lorson, H. Rindt, M. Shababi, Spinal muscular atrophy: Mechanisms and therapeutic strategies. *Hum. Mol. Genet.* **19**, R111–R118 (2010).
6. D. D. Coovert *et al.*, The survival motor neuron protein in spinal muscular atrophy. *Hum. Mol. Genet.* **6**, 1205–1214 (1997).
7. S. Lefebvre *et al.*, Identification and characterization of a spinal muscular atrophy-determining gene. *Cell* **80**, 155–165 (1995).
8. S. Lefebvre *et al.*, Correlation between severity and SMN protein level in spinal muscular atrophy. *Nat. Genet.* **16**, 265–269 (1997).
9. C. L. Lorson, E. Hahnen, E. J. Androphy, B. Wirth, A single nucleotide in the SMN gene regulates splicing and is responsible for spinal muscular atrophy. *Proc. Natl. Acad. Sci. U.S.A.* **96**, 6307–6311 (1999).
10. C. J. DiDonato *et al.*, Regulation of murine survival motor neuron (Smn) protein levels by modifying Smn exon 7 splicing. *Hum. Mol. Genet.* **10**, 2727–2736 (2001).
11. B. Akten *et al.*, Interaction of survival of motor neuron (SMN) and HuD proteins with mRNA cpg15 rescues motor neuron axonal deficits. *Proc. Natl. Acad. Sci. U.S.A.* **108**, 10337–10342 (2011).
12. L. Pellizzoni, J. Yong, G. Dreyfuss, Essential role for the SMN complex in the specificity of snRNP assembly. *Science* **298**, 1775–1779 (2002).
13. W. Rossoll *et al.*, Smn, the spinal muscular atrophy-determining gene product, modulates axon growth and localization of beta-actin mRNA in growth cones of motoneurons. *J. Cell Biol.* **163**, 801–812 (2003).
14. M. L. McWhorter, U. R. Monani, A. H. Burghes, C. E. Beattie, Knockdown of the survival motor neuron (Smn) protein in zebrafish causes defects in motor axon outgrowth and pathfinding. *J. Cell Biol.* **162**, 919–931 (2003).
15. G. Meister, D. Buhler, R. Pillai, F. Lottspeich, U. Fischer, A multiprotein complex mediates the ATP-dependent assembly of spliceosomal U snRNPs. *Nat. Cell Biol.* **3**, 945–949 (2001).
16. Z. Zhang *et al.*, SMN deficiency causes tissue-specific perturbations in the repertoire of snRNAs and widespread defects in splicing. *Cell* **133**, 585–600 (2008).
17. D. Baumer *et al.*, Alternative splicing events are a late feature of pathology in a mouse model of spinal muscular atrophy. *PLoS Genet.* **5**, e1000773 (2009).
18. K. K. Ling, M. Y. Lin, B. Zingg, Z. Feng, C. P. Ko, Synaptic defects in the spinal and neuromuscular circuitry in a mouse model of spinal muscular atrophy. *PLoS One* **5**, e15457 (2010).
19. S. Kariya *et al.*, Reduced SMN protein impairs maturation of the neuromuscular junctions in mouse models of spinal muscular atrophy. *Hum. Mol. Genet.* **17**, 2552–2569 (2008).
20. G. Z. Mentis *et al.*, Early functional impairment of sensory-motor connectivity in a mouse model of spinal muscular atrophy. *Neuron* **69**, 453–467 (2011).
21. V. L. McGovern, T. O. Gavrilina, C. E. Beattie, A. H. Burghes, Embryonic motor axon development in the severe SMA mouse. *Hum. Mol. Genet.* **17**, 2900–2909 (2008).
22. N. Miller, H. Shi, A. S. Zelikovich, Y. C. Ma, Motor neuron mitochondrial dysfunction in spinal muscular atrophy. *Hum. Mol. Genet.* **25**, 3395–3406 (2016).
23. P. J. Boyd *et al.*, Bioenergetic status modulates motor neuron vulnerability and pathogenesis in a zebrafish model of spinal muscular atrophy. *PLoS Genet.* **13**, e1006744 (2017).
24. Y. Hua *et al.*, Peripheral SMN restoration is essential for long-term rescue of a severe spinal muscular atrophy mouse model. *Nature* **478**, 123–126 (2011).
25. K. D. Foust *et al.*, Rescue of the spinal muscular atrophy phenotype in a mouse model by early postnatal delivery of SMN. *Nat. Biotechnol.* **28**, 271–274 (2010).
26. N. A. Naryshkin *et al.*, Motor neuron disease. SMN2 splicing modifiers improve motor function and longevity in mice with spinal muscular atrophy. *Science* **345**, 688–693 (2014).
27. M. Van Alstyne *et al.*, Gain of toxic function by long-term AAV9-mediated SMN overexpression in the sensorimotor circuit. *Nat. Neurosci.* **24**, 930–940 (2021).
28. Z. H. Cheung, N. Y. Ip, Cdk5: A multifaceted kinase in neurodegenerative diseases. *Trends Cell Biol.* **22**, 169–175 (2012).
29. S. C. Su, L. H. Tsai, Cyclin-dependent kinases in brain development and disease. *Annu. Rev. Cell Dev. Biol.* **27**, 465–491 (2011), 10.1146/annurev-cellbio-092910-154023.
30. E. Klinman, E. L. Holzbaur, Stress-induced CDK5 activation disrupts axonal transport via Lis1/Ndel1/dynein. *Cell Rep.* **12**, 462–473 (2015).
31. Z. H. Cheung, A. K. Fu, N. Y. Ip, Synaptic roles of Cdk 5: Implications in higher cognitive functions and neurodegenerative diseases. *Neuron* **50**, 13–18 (2006).
32. Z. H. Cheung, K. Gong, N. Y. Ip, Cyclin-dependent kinase 5 supports neuronal survival through phosphorylation of Bcl-2. *J. Neurosci.* **28**, 4872–4877 (2008).
33. L. Shi, A. K. Fu, N. Y. Ip, Molecular mechanisms underlying maturation and maintenance of the vertebrate neuromuscular junction. *Trends Neurosci.* **35**, 441–453 (2012).
34. A. S. Wong *et al.*, Cdk5-mediated phosphorylation of endophilin B1 is required for induced autophagy in models of Parkinson's disease. *Nat. Cell Biol.* **13**, 568–579 (2011).
35. A. K. Fu *et al.*, Cdk5 is involved in neuregulin-induced AChR expression at the neuromuscular junction. *Nat. Neurosci.* **4**, 374–381 (2001).
36. K. O. Lai *et al.*, TrkB phosphorylation by Cdk5 is required for activity-dependent structural plasticity and spatial memory. *Nat. Neurosci.* **15**, 1506–1515 (2012), 10.1038/nn.3237.
37. J. P. Pandey, D. S. Smith, A Cdk5-dependent switch regulates Lis1/Ndel1/dynein-driven organelle transport in adult axons. *J. Neurosci.* **31**, 17207–17219 (2011).
38. T. B. Shea *et al.*, Cdk5 regulates axonal transport and phosphorylation of neurofilaments in cultured neurons. *J. Cell Sci.* **117**, 933–941 (2004).
39. L. H. Tsai, I. Delalle, V. S. Caviness Jr., T. Chae, E. Harlow, p35 is a neural-specific regulatory subunit of cyclin-dependent kinase 5. *Nature* **371**, 419–423 (1994).
40. J. Lew *et al.*, A brain-specific activator of cyclin-dependent kinase 5. *Nature* **371**, 423–426 (1994).
41. C. Y. Ou *et al.*, Two cyclin-dependent kinase pathways are essential for polarized trafficking of presynaptic components. *Cell* **141**, 846–858 (2010).
42. W. Lin *et al.*, Neurotransmitter acetylcholine negatively regulates neuromuscular synapse formation by a Cdk5-dependent mechanism. *Neuron* **46**, 569–579 (2005).
43. M. D. Nguyen, R. C. Lariviere, J. P. Julien, Deregulation of Cdk5 in a mouse model of ALS: Toxicity alleviated by perikaryal neurofilament inclusions. *Neuron* **30**, 135–147 (2001).
44. G. N. Patrick *et al.*, Conversion of p35 to p25 deregulates Cdk5 activity and promotes neurodegeneration. *Nature* **402**, 615–622 (1999).
45. B. Bu, J. Li, P. Davies, I. Vincent, Deregulation of cdk5, hyperphosphorylation, and cytoskeletal pathology in the Niemann-Pick type C murine model. *J. Neurosci.* **22**, 6515–6525 (2002).
46. P. D. Smith *et al.*, Calpain-regulated p35/cdk5 plays a central role in dopaminergic neuron death through modulation of the transcription factor myocyte enhancer factor 2. *J. Neurosci.* **26**, 440–447 (2006).
47. J. Ko *et al.*, p35 and p39 are essential for cyclin-dependent kinase 5 function during neurodevelopment. *J. Neurosci.* **21**, 6758–6771 (2001).
48. D. Tang *et al.*, An isoform of the neuronal cyclin-dependent kinase 5 (Cdk5) activator. *J. Biol. Chem.* **270**, 26897–26903 (1995).
49. M. Zheng, C. L. Leung, R. K. Liem, Region-specific expression of cyclin-dependent kinase 5 (cdk5) and its activators, p35 and p39, in the developing and adult rat central nervous system. *J. Neurobiol.* **35**, 141–159 (1998).
50. K. Tomizawa *et al.*, Localization and developmental changes in the neuron-specific cyclin-dependent kinase 5 activator (p35nck5a) in the rat brain. *Neuroscience* **74**, 519–529 (1996).
51. G. Kusakawa *et al.*, Calpain-dependent proteolytic cleavage of the p35 cyclin-dependent kinase 5 activator to p25. *J. Biol. Chem.* **275**, 17166–17172 (2000).
52. M. S. Lee *et al.*, Neurotoxicity induces cleavage of p35 to p25 by calpain. *Nature* **405**, 360–364 (2000).
53. J. C. Cruz *et al.*, p25/cyclin-dependent kinase 5 induces production and intraneuronal accumulation of amyloid beta in vivo. *J. Neurosci.* **26**, 10536–10541 (2006).
54. C. Otth *et al.*, AbetaPP induces cdk5-dependent tau hyperphosphorylation in transgenic mice Tg2576. *J. Alzheimers Dis.* **4**, 417–430 (2002).
55. A. K. Fu *et al.*, Aberrant motor axon projection, acetylcholine receptor clustering, and neurotransmission in cyclin-dependent kinase 5 null mice. *Proc. Natl. Acad. Sci. U.S.A.* **102**, 15224–15229 (2005).
56. N. Miller *et al.*, Non-aggregating tau phosphorylation by cyclin-dependent kinase 5 contributes to motor neuron degeneration in spinal muscular atrophy. *J. Neurosci.* **35**, 6038–6050 (2015).
57. T. T. Le *et al.*, SMNDelta7, the major product of the centromeric survival motor neuron (SMN2) gene, extends survival in mice with spinal muscular atrophy and associates with full-length SMN. *Hum. Mol. Genet.* **14**, 845–857 (2005).
58. H. M. Hsieh-Li *et al.*, A mouse model for spinal muscular atrophy. *Nat. Genet.* **24**, 66–70 (2000).
59. Y. C. Ma, J. Huang, S. Ali, W. Lowry, X. Y. Huang, Src tyrosine kinase is a novel direct effector of G proteins. *Cell* **102**, 635–646 (2000).
60. L. H. Tsai, T. Takahashi, V. S. Caviness Jr., E. Harlow, Activity and expression pattern of cyclin-dependent kinase 5 in the embryonic mouse nervous system. *Development* **119**, 1029–1040 (1993).
61. A. D. Ebert *et al.*, Induced pluripotent stem cells from a spinal muscular atrophy patient. *Nature* **457**, 277–280 (2009).
62. D. Sareen *et al.*, Inhibition of apoptosis blocks human motor neuron cell death in a stem cell model of spinal muscular atrophy. *PLoS One* **7**, e39113 (2012).
63. H. Wichterle, I. Lieberam, J. A. Porter, T. M. Jessell, Directed differentiation of embryonic stem cells into motor neurons. *Cell* **110**, 385–397 (2002).
64. T. Ohshima *et al.*, Targeted disruption of the cyclin-dependent kinase 5 gene results in abnormal corticogenesis, neuronal pathology and perinatal death. *Proc. Natl. Acad. Sci. U.S.A.* **93**, 11173–11178 (1996).
65. T. Chae *et al.*, Mice lacking p35, a neuronal specific activator of Cdk5, display cortical lamination defects, seizures, and adult lethality. *Neuron* **18**, 29–42 (1997).
66. A. Jahani-Asl *et al.*, CDK5 phosphorylates DRP1 and drives mitochondrial defects in NMDA-induced neuronal death. *Hum. Mol. Genet.* **24**, 4573–4583 (2015).
67. L. D. Aarreberg *et al.*, Interleukin-1beta induces mtDNA release to activate innate immune signaling via cGAS-STING. *Mol. Cell* **74**, 801–815.e6 (2019).
68. H. Chen, D. C. Chan, Critical dependence of neurons on mitochondrial dynamics. *Curr. Opin. Cell Biol.* **18**, 453–459 (2006).
69. K. K. Ling, R. M. Gibbs, Z. Feng, C. P. Ko, Severe neuromuscular denervation of clinically relevant muscles in a mouse model of spinal muscular atrophy. *Hum. Mol. Genet.* **21**, 185–195 (2012).

70. L. Kong *et al.*, Impaired synaptic vesicle release and immaturity of neuromuscular junctions in spinal muscular atrophy mice. *J. Neurosci.* **29**, 842–851 (2009).
71. L. M. Murray *et al.*, Selective vulnerability of motor neurons and dissociation of pre- and post-synaptic pathology at the neuromuscular junction in mouse models of spinal muscular atrophy. *Hum. Mol. Genet.* **17**, 949–962 (2008).
72. X. Paez-Colasante *et al.*, Improvement of neuromuscular synaptic phenotypes without enhanced survival and motor function in severe spinal muscular atrophy mice selectively rescued in motor neurons. *PLoS One* **8**, e75866 (2013).
73. S. Rudnik-Schoneborn *et al.*, Congenital heart disease is a feature of severe infantile spinal muscular atrophy. *J. Med. Genet.* **45**, 635–638 (2008).
74. A. K. Bevan *et al.*, Early heart failure in the SMNDelta7 model of spinal muscular atrophy and correction by postnatal scAAV9-SMN delivery. *Hum. Mol. Genet.* **19**, 3895–3905 (2010).
75. C. R. Heier, R. Satta, C. Lutz, C. J. DiDonato, Arrhythmia and cardiac defects are a feature of spinal muscular atrophy model mice. *Hum. Mol. Genet.* **19**, 3906–3918 (2010).
76. M. Shababi *et al.*, Cardiac defects contribute to the pathology of spinal muscular atrophy models. *Hum. Mol. Genet.* **19**, 4059–4071 (2010).
77. G. Hamilton, T. H. Gillingwater, Spinal muscular atrophy: Going beyond the motor neuron. *Trends Mol. Med.* **19**, 40–50 (2013).
78. M. O. Deguise *et al.*, Immune dysregulation may contribute to disease pathogenesis in spinal muscular atrophy mice. *Hum. Mol. Genet.* **26**, 801–819 (2017).
79. M. Gou-Fabregas *et al.*, Specific vulnerability of mouse spinal cord motoneurons to membrane depolarization. *J. Neurochem.* **110**, 1842–1854 (2009).
80. T. Tsujinaka *et al.*, Synthesis of a new cell penetrating calpain inhibitor (calpeptin). *Biochem. Biophys. Res. Commun.* **153**, 1201–1208 (1988).
81. A. Kazmierczak, G. A. Czapski, A. Adamczyk, B. Gajkowska, J. B. Strosznajder, A novel mechanism of non-Abeta component of Alzheimer's disease amyloid (NAC) neurotoxicity. Interplay between p53 protein and cyclin-dependent kinase 5 (Cdk5). *Neurochem. Int.* **58**, 206–214 (2011).
82. S. K. Ray, G. G. Wilford, D. C. Matzelle, E. L. Hogan, N. L. Banik, Calpeptin and methylprednisolone inhibit apoptosis in rat spinal cord injury. *Ann. N. Y. Acad. Sci.* **890**, 261–269 (1999).
83. Z. H. Sheng, Q. Cai, Mitochondrial transport in neurons: Impact on synaptic homeostasis and neurodegeneration. *Nat. Rev. Neurosci.* **13**, 77–93 (2012).
84. J. S. Kang *et al.*, Docking of axonal mitochondria by syntaphilin controls their mobility and affects short-term facilitation. *Cell* **132**, 137–148 (2008).
85. X. Wang, T. L. Schwarz, The mechanism of Ca2+ -dependent regulation of kinesin-mediated mitochondrial motility. *Cell* **136**, 163–174 (2009).
86. L. Pellizzoni, N. Kataoka, B. Charroux, G. Dreyfuss, A novel function for SMN, the spinal muscular atrophy disease gene product, in pre-mRNA splicing. *Cell* **95**, 615–624 (1998).
87. T. K. Doktor *et al.*, RNA-sequencing of a mouse-model of spinal muscular atrophy reveals tissue-wide changes in splicing of U12-dependent introns. *Nucleic Acids Res.* **45**, 395–416 (2017), 10.1093/nar/gkw731.
88. F. Lotti *et al.*, An SMN-dependent U12 splicing event essential for motor circuit function. *Cell* **151**, 440–454 (2012).
89. R. Tejero *et al.*, R-roscovitine improves motoneuron function in mouse models for spinal muscular atrophy. *iScience* **23**, 100826 (2020).
90. X. Gong *et al.*, Cdk5-mediated inhibition of the protective effects of transcription factor MEF2 in neurotoxicity-induced apoptosis. *Neuron* **38**, 33–46 (2003).
91. K. Baumann, E. M. Mandelkow, J. Biernat, H. Piwnica-Worms, E. Mandelkow, Abnormal Alzheimer-like phosphorylation of tau-protein by cyclin-dependent kinases cdk2 and cdk5. *FEBS Lett.* **336**, 417–424 (1993).
92. R. Dixit, J. L. Ross, Y. E. Goldman, E. L. Holzbaur, Differential regulation of dynein and kinesin motor proteins by tau. *Science* **319**, 1086–1089 (2008).
93. A. Ebneth *et al.*, Overexpression of tau protein inhibits kinesin-dependent trafficking of vesicles, mitochondria, and endoplasmic reticulum: Implications for Alzheimer's disease. *J. Cell Biol.* **143**, 777–794 (1998).
94. G. Lee, S. T. Newman, D. L. Gard, H. Band, G. Panchamoorthy, Tau interacts with src-family non-receptor tyrosine kinases. *J. Cell Sci.* **111**, 3167–3177 (1998).
95. C. H. Reynolds *et al.*, Phosphorylation regulates tau interactions with Src homology 3 domains of phosphatidylinositol 3-kinase, phospholipase Cgamma1, Grb2, and Src family kinases. *J. Biol. Chem.* **283**, 18177–18186 (2008).
96. M. Morris, S. Maeda, K. Vossel, L. Mucke, The many faces of tau. *Neuron* **70**, 410–426 (2011).
97. L. M. Ittner *et al.*, Dendritic function of tau mediates amyloid-beta toxicity in Alzheimer's disease mouse models. *Cell* **142**, 387–397 (2010).
98. S. W. Flavell *et al.*, Activity-dependent regulation of MEF2 transcription factors suppresses excitatory synapse number. *Science* **311**, 1008–1012 (2006).
99. Z. Mao, A. Bonni, F. Xia, M. Nadal-Vicens, M. E. Greenberg, Neuronal activity-dependent cell survival mediated by transcription factor MEF2. *Science* **286**, 785–790 (1999).
100. S. W. Flavell *et al.*, Genome-wide analysis of MEF2 transcriptional program reveals synaptic target genes and neuronal activity-dependent polyadenylation site selection. *Neuron* **60**, 1022–1038 (2008).
101. A. Shalizi *et al.*, A calcium-regulated MEF2 sumoylation switch controls postsynaptic differentiation. *Science* **311**, 1012–1017 (2006).
102. A. E. West, E. C. Griffith, M. E. Greenberg, Regulation of transcription factors by neuronal activity. *Nat. Rev. Neurosci.* **3**, 921–931 (2002).
103. H. She *et al.*, Direct regulation of complex I by mitochondrial MEF2D is disrupted in a mouse model of Parkinson disease and in human patients. *J. Clin. Invest.* **121**, 930–940 (2011).
104. K. R. Pryde, J. Hirst, Superoxide is produced by the reduced flavin in mitochondrial complex I: A single, unified mechanism that applies during both forward and reverse electron transfer. *J. Biol. Chem.* **286**, 18056–18065 (2011).
105. Y. Kushnareva, A. N. Murphy, A. Andreyev, Complex I-mediated reactive oxygen species generation: Modulation by cytochrome c and NAD(P)+ oxidation-reduction state. *Biochem. J.* **368**, 545–553 (2002).
106. C. d'Ydewalle *et al.*, The antisense transcript SMN-AS1 regulates SMN expression and is a novel therapeutic target for spinal muscular atrophy. *Neuron* **93**, 66–79 (2017).
107. P. S. Vosler, C. S. Brennan, J. Chen, Calpain-mediated signaling mechanisms in neuronal injury and neurodegeneration. *Mol. Neurobiol.* **38**, 78–100 (2008).
108. Y. Wen *et al.*, Interplay between cyclin-dependent kinase 5 and glycogen synthase kinase 3 beta mediated by neuregulin signaling leads to differential effects on tau phosphorylation and amyloid precursor protein processing. *J. Neurosci.* **28**, 2624–2632 (2008).
109. S. Lapenna, A. Giordano, Cell cycle kinases as therapeutic targets for cancer. *Nat. Rev. Drug Discov.* **8**, 547–566 (2009).
110. J. R. Sundaram *et al.*, Specific inhibition of p25/Cdk5 activity by the Cdk5 inhibitory peptide reduces neurodegeneration in vivo. *J. Neurosci.* **33**, 334–343 (2013).
111. Y. L. Zheng *et al.*, A Cdk5 inhibitory peptide reduces tau hyperphosphorylation and apoptosis in neurons. *EMBO J.* **24**, 209–220 (2005).
112. Y. L. Zheng, B. S. Li, N. D. Amin, W. Albers, H. C. Pant, A peptide derived from cyclin-dependent kinase activator (p35) specifically inhibits Cdk5 activity and phosphorylation of tau protein in transfected cells. *Eur. J. Biochem.* **269**, 4427–4434 (2002).
113. K. A. Quinlan, J. E. Schuster, R. Fu, T. Siddique, C. J. Heckman, Altered postnatal maturation of electrical properties in spinal motoneurons in a mouse model of amyotrophic lateral sclerosis. *J. Physiol.* **589**, 2245–2260 (2011).